VARIABILITY OF BASAL GANGLIA MORPHOLOGY AFTER SPATIAL NORMALIZATION: IMPLICATIONS FOR GROUP STUDIES

Jingyun Chen[1], Martin J. McKeown[2], Mirza Faisal Beg[1]
[1]Medical Image Analysis Lab, School of Engineering Science, Simon Fraser University.
[2]Pacific Parkinson's Research Centre, University of British Columbia

INTRODUCTION

In neuroimaging, spatial normalization refers to spatially transforming different brain MR scans to a standard space for purposes of atlas alignment, inter-subject averaging, or characterization of anatomical structures. In fMRI analyses, time series from different subjects are concatenated together under the assumption that there is a perfect correspondence at the voxel level across subjects after normalization. Often data are spatially smoothed to make this assumption less rigid, but this degrades the spatial resolution. Standard low dimensional methods for spatial normalization can result in significant mis-registration, particularly for smaller structures such as those of the basal ganglia. The aim of this paper is to rigorously assess the residual anatomical variability (RAV) in basal ganglia structures after standard spatial normalization. This has profound implications for group studies in populations where the basal ganglia are being examined, e.g. Parkinson's Disease.

We studied the extent of RAV in basal ganglia structures in 27 T1-weighted brain scans after spatial normalization by different methods. Specifically, we assessed the normalization performance of Freesurfer[1], Statistical Parametric Mapping (SPM)[2], and Large Deformation Diffeomorphic Metric Mapping (LDDMM)[3]. We specifically concentrated on basal ganglia structures in each hemisphere were considered. As expected, smaller ROIs had increased RAV when computed over all subject pairs with different group sizes and registration methods. The LDDMM method had the lowest RAV of the three methods, but was the most computationally intensive. This result has major implications for group fMRI studies that utilize spatial normalization as a standard pre-processing method, and supports the use of fMRI ROI analysis methods that compute significance in each subject's native space, especially when basal ganglia structures are involved.

The rest of the paper is organized as follows. In the second section, details of the data and methods are introduced. In the third section, data processing results with the different methods are presented and discussed. Finally in the fourth section the experiment results are concluded.

METHODS

We assessed RAV in this paper with the following three steps:

1) Data acquisition: We acquired 27 T1-weighted brain MR images from a 3 Tesla scanner (Philips Achieva 3.0T; Philips Medical Systems, Netherlands), with 170 slices axially parallel to the AC-PC plane. The subject cohort consists of two groups: 14 Parkinson's Disease (PD) subjects and 13 age-matched control subjects with no known neurological or psychiatric conditions. Four basal ganglia ROIs (putamen, caudate, thalamus, globus pallidus) in each hemisphere were outlined manually by a trained research assistant using Amira software (Amira 3D Visualization and Volume Modeling V.3.1.1.), as shown in Figure 1.
2) Spatial Normalization: Three different registration tools were used to normalize the ROIs of each subject. A) The 12-parameter affine registration to the Talairach space[5] implemented in Freesurfer work flow (autorecon1). B) SPM's default spatial normalise module, including affine and 7x8x7 nonlinear basis functions. C) Freesurfer-initialized LDDMM (FS+LDDMM) registration[4], with the deformation fields applied to the ROIs of each subject.
3) Variability Measurement: We used the Dice similarity coefficients (DSC) to measure the overlap percentage of normalized ROIs under template space. The DSC is defined as:

$$DSC = n \times V(\bigcap_{i} S_i) / \sum_{i=1}^{n} V(S_i) \quad (1)$$

where S_i, $(i=1,2\ldots n)$ are ROIs in this paper. $V(S_i)$ is the number of non-zero voxels of of S_i (i.e. the volume of ROI S_i), and n is the number of subjects to overlay, which we will refer to as the group size. When $n=2$, $DSC(A,B)=2V(A \cap B)/[V(A)+V(B)]$, a measure commonly used to assess segmentation similarity, sometimes referred to as the similarity index (SI), Kappa coefficient, or mean overlap. For

complete overlap between two segmentations, *DSC*=1, and for no overlap, DSC=0. We computed the average DSC of normalized ROIs using Nieto-Castanon's scheme[6]. Average DSCs were computed over all possible subject combinations.

RESULTS

The average DSCs of ROIs after three different spatial normalization methods are shown in Figure 2. For subject group size=2 the DSCs (average ± standard deviation) are shown in Table 1. In all the experiments average DSC generally decreases as subject group size increases. The average DSC with the FS+LDDMM registration was less than the other two methods. Among the 4 basal ganglia ROIs, the average DSCs of the globus pallidi was significantly lower than the other 3 ROIs. This is mainly because the number of voxels contained within the globus pallidus tends to be smaller than other ROIs, and therefore has a higher proportion of boundary voxels.

To estimate the manual segmentation variability of the ROIs, one subject from the control group was manually segmented 5 times by the same person. The DSCs (average ± standard deviation, subject group size=2) for the four ROIs are shown in Table 1. The high average DSCs and low standard deviation indicates that the manual segmentation is generally consistent, and therefore the RAV mainly arises from misregistrations after the spatial normalization process.

CONCLUSION

Spatial normalization is extensively used for atlas alignment, inter-subject averaging, and anatomical characterization, and has been integrated into many MR study tools. However, evidence in this paper indicates that for low dimensional registration methods, misregistration, particularly as the group sizes increase, is a particular problem for basal ganglia structures. A high-dimensional registration method such as LDDMM is necessary to reduce the anatomical variability before further processing.

Compared to the recent papers quantifying RAV of different registration techniques[7,8,9], this paper contains the following novel work.

1) We focused on the RAV of four PD-related basal ganglia structures after whole brain spatial normalization.
2) We quantified the influence of subject group size on RAV of the subjects after spatial normalization. Other factors with potential influences to RAV, such as consistency of ROI segmentation and neurological or psychiatric conditions of subjects were also studied.

FIGURE AND TABLES

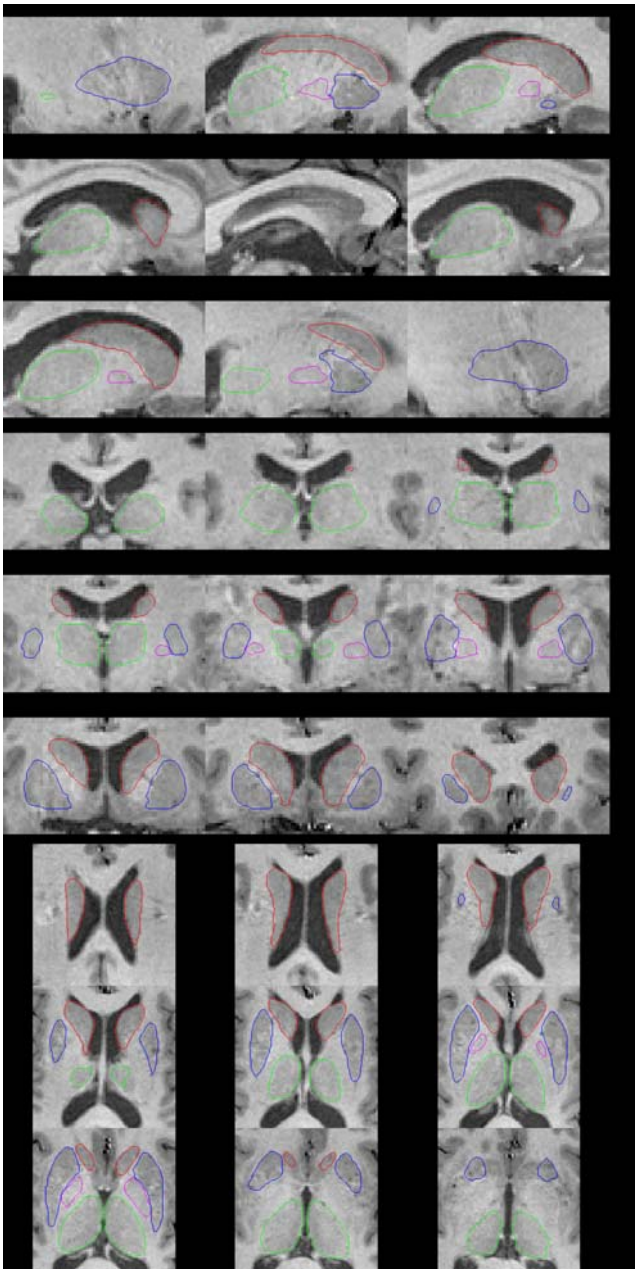

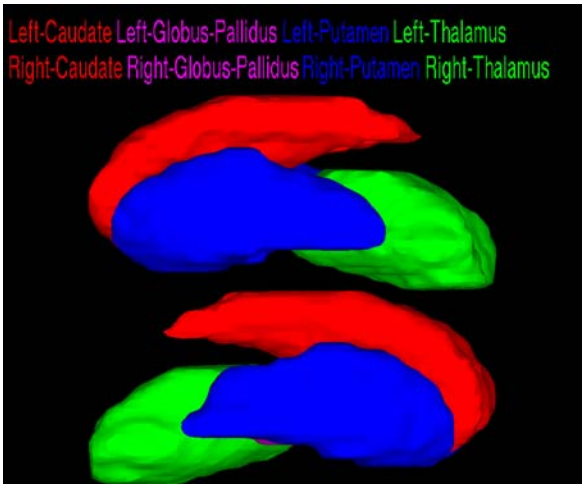

Figure 1: Outlines of ROIs on the structural image. The 3x3 image array on the top is sagittal view, the second array from top is coronal view, the one below that is transverse view. One the bottom are the colorfully rendered ROI surfaces with differe, red-caudate, blue-putamen, green-thalamus and pink-globus-pallidus

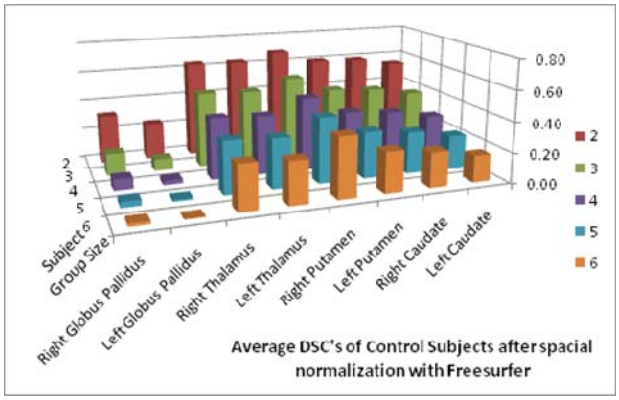

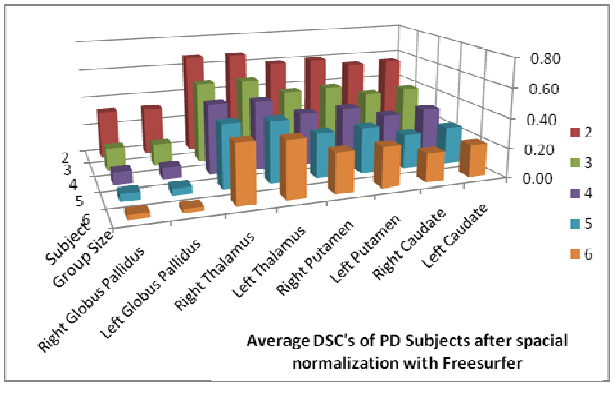

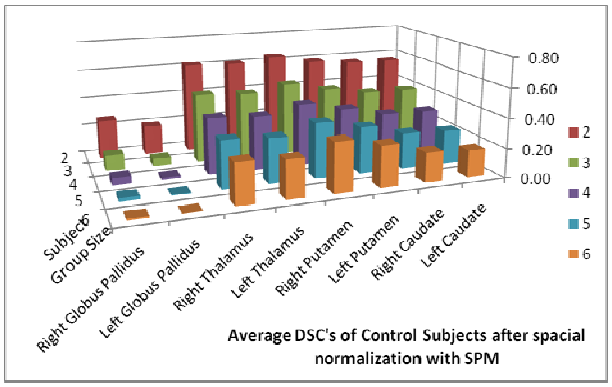

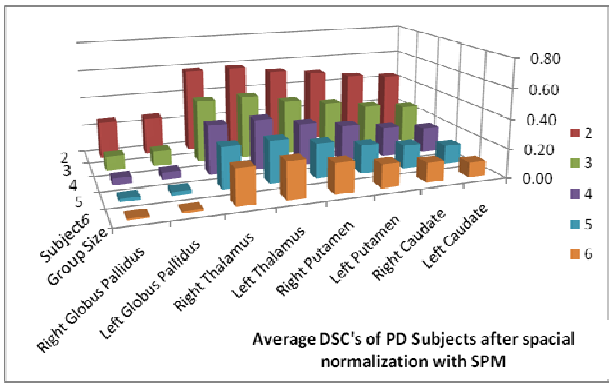

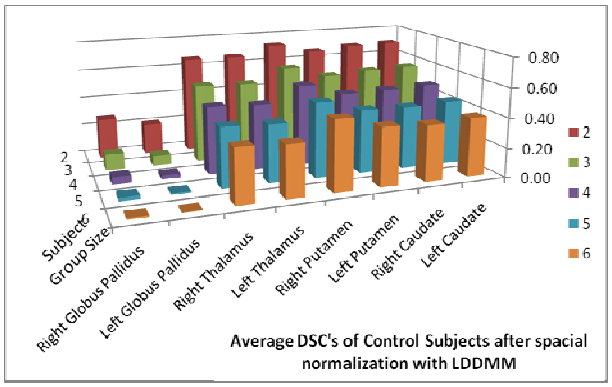

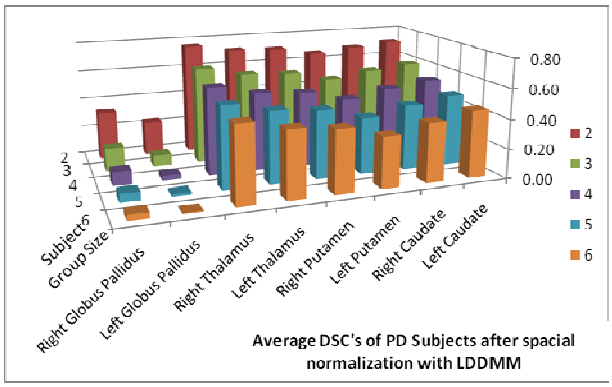

Figure 2: Average DSCs with different spatial normalization methods

.

Table 1: DSCs (average ± standard deviation) with subject group size=2

ROI	Manual	FS+LDDMM	FS	SPM
Left Caudate	0.87±0.02	0.7±0.03	0.55±0.05	0.56±0.06
Right Caudate	0.85±0.02	0.69±0.03	0.59±0.05	0.57±0.05
Left Putamen	0.84±0.03	0.67±0.04	0.60±0.07	0.59±0.07
Right Putamen	0.86±0.03	0.73±0.04	0.68±0.07	0.64±0.07
Left Thalamus	0.87±0.2	0.66±0.03	0.64±0.06	0.61±0.06
Right Thalamus	0.85±0.02	0.66±0.02	0.64±0.05	0.62±0.06
Left Pallidum	0.69±0.01	0.21±0.01	0.24±0.05	0.20±0.04
Right Pallidum	0.55±0.01	0.27±0.02	0.32±0.04	0.27±0.04

REFERENCES

[1] J. Ashburner, K. J. Friston,, "Nonlinear spatial normalization using basis functions". *Human Brain Mapping*, vol. 7, pp.254-266, 1999.

[2] B. Fischl et al., "Whole brain segmentation: automated labeling of neuroanatomical structures in the human brain", *Neuron,* vol. 33, pp. 341-355, 2002.

[3] M. F. Beg, M. I. Miller, A. Trouve, L. Younes, "Computing large deformation metric mappings via geodesic flows of diffeomorphisms", *International Journal of Computer. Vision*, vol. 61(2), pp.139-157, 2005

[4] A. R. Khan, L. Wang, M. F. Beg, "Freesurfer-initiated fully-automated subcortical brain segmentation in mri using large deformation diffeomorphic metric mapping", *NeuroImage*, vol. 41(3), pp. 735-746, 2008.

[5] D. L. Collins, P. Neelin, T. M. Peters and A. C. Evans, "Automatic 3D inter-subject registration of MR volumetric data in standardized Talairach space", *Journal of Computer Assisted Tomography*, vol. 18(2) pp. 192-205, ,1994.

[6] A. Nieto-Castanon, S. S. Ghosh, J. A. Tourville, F. H. Guenther, "Region of interest based analysis of functional imaging data", *NeuroImage*, vol. 19(4), pp. 1303-1316, 2003.

[7] M. A. Yassa, and C. E. L. Stark, "A quantitative evaluation of cross-participant registration techniques for MRI studies of the medial temporal lobe", *Neuroimage*, vol. 44 (2), pp. 319-327, 2009

[8] M. Wu et al., "Quantitative comparison of AIR, SPM, and the fully deformable model for atlas-based segmentation of functional and structural MR images", *Human Brain Mapping*, vol. 27(9), pp. 747-754, 2006.

[9] A. Klein et al., "Evaluation of 14 nonlinear deformation algorithms applied to human brain MRI registration", *Neuroimage*, vol. 46(3), pp.786-802, 2009.